



# On the superior activity and selectivity of PtCo/Nb<sub>2</sub>O<sub>5</sub> Fischer Tropsch catalysts



J.H. den Otter<sup>a</sup>, H. Yoshida<sup>b</sup>, C. Ledesma<sup>c</sup>, D. Chen<sup>c</sup>, K.P. de Jong<sup>a,\*</sup>

<sup>a</sup> Inorganic Chemistry and Catalysis, Debye Institute for Nanomaterials Science, Utrecht University, Universiteitsweg 99, 3584 CG Utrecht, The Netherlands

<sup>b</sup> The Institute of Scientific and Industrial Research, Osaka University, 8-1 Mihogaoka, Ibaraki, Osaka 567-0047, Japan

<sup>c</sup> Department of Chemical Engineering, Norwegian University of Science and Technology, Sem Sælands vei 4, N-7491 Trondheim, Norway

## ARTICLE INFO

### Article history:

Received 2 February 2016

Revised 25 May 2016

Accepted 29 May 2016

Available online 21 June 2016

### Keywords:

Fischer Tropsch

Niobia

Activity promotion

TOF

Noble metal

## ABSTRACT

In this study Co/Nb<sub>2</sub>O<sub>5</sub> catalysts and the effect of Pt-promotion thereon are investigated in comparison with  $\gamma$ -Al<sub>2</sub>O<sub>3</sub>- and  $\alpha$ -Al<sub>2</sub>O<sub>3</sub>-supported catalysts for the Fischer Tropsch (FT) synthesis. Upon Pt-promotion of Co/Nb<sub>2</sub>O<sub>5</sub> the cobalt-weight normalized FT activity was found to increase by a factor of 2.4, while the high C<sub>5+</sub> selectivity of 85 wt% was maintained. Based on environmental TEM results no indications were found that Pt affected the cobalt particle size in Co/Nb<sub>2</sub>O<sub>5</sub> catalysts. A kinetic study indicates an increased number of active sites upon Pt-promotion whereas Steady-State Isotopic Transient Kinetic Analysis experiments show that a combination of an increased number of active sites and an increased turnover frequency is at the origin of the enhanced activity in Co/Nb<sub>2</sub>O<sub>5</sub> catalysts upon Pt-promotion. Pt was tentatively proposed to bring about more efficient promotion of Co by NbO<sub>x</sub> being present as smaller clusters.

© 2016 Elsevier Inc. All rights reserved.

## 1. Introduction

The price of crude oil and the call for cleaner transportation fuels have stimulated the development of methods to synthesize liquid hydrocarbons from alternative carbon feedstocks such as natural gas, coal and biomass which can be converted into syngas, a mixture of CO and H<sub>2</sub>. Via the Fischer Tropsch reaction, typically catalyzed by iron or cobalt catalysts, hydrocarbons can be produced from syngas and can be used as high-quality transportation fuels or chemicals. Iron catalysts at high temperatures are typically used for the synthesis of lower olefins [1], whereas silica-, alumina- or titania-supported cobalt catalysts at low temperatures give rise to heavy hydrocarbons [2–5].

The selectivity of cobalt catalysts toward liquid hydrocarbons (C<sub>5+</sub>) is affected by process conditions such as temperature [6,7], pressure [8] and CO conversion [9] and catalyst properties such as support acidity [10,11] and pore diameter [5,10] and can be promoted by partially reducible transition metal oxides such as MnO and ZrO<sub>2</sub> [12–17]. These promoters can be present as small particles in the close proximity to cobalt or as support material in the case of Co/TiO<sub>2</sub> [16,18,19] or Co/Nb<sub>2</sub>O<sub>5</sub> [6,20–24] catalysts. For Nb<sub>2</sub>O<sub>5</sub>-supported cobalt catalysts, high selectivities toward heavy

hydrocarbons were reported at 1 bar by Schmal and coworkers [20–24] and more recently at 20 bar by den Otter et al. [6]. The promoting effect of niobia as support material at low pressure was extensively studied by XPS, TPR, TPO, CO TPD and IR spectroscopy and was attributed to partial reduction of the support and consequent strong metal support interaction (SMSI) [25–29]. The presence of Co<sup>0</sup>-NbO<sub>x</sub> species was confirmed by Mendes et al. in Co/Nb<sub>2</sub>O<sub>5</sub> catalysts [27] and model catalysts [28].

Noble-metal addition is a well-known method to enhance the activity of Fischer Tropsch catalysts by facilitating cobalt oxide reduction and consequently increasing the number of active sites [30–33]. During Fischer–Tropsch catalysis, Pt is not expected to be active as catalyst due to the low CO dissociation activity; however, it might assist by facilitating H<sub>2</sub> dissociation or act as adsorption site for CO [34]. Upon noble metal promotion of Co/TiO<sub>2</sub> and Co/Nb<sub>2</sub>O<sub>5</sub> catalysts [2,35–37] and recently also niobia-promoted Co/SiO<sub>2</sub> catalysts [8], an increase in the cobalt-weight normalized activity was observed which could not be explained only by an increased number of active sites.

In this study the extent and origin of Pt-promotion on the activity and selectivity of Co/Nb<sub>2</sub>O<sub>5</sub> Fischer Tropsch catalysts are investigated in comparison with  $\gamma$ -Al<sub>2</sub>O<sub>3</sub>- and  $\alpha$ -Al<sub>2</sub>O<sub>3</sub>-supported catalysts using among other environmental Transmission Electron Microscopy (TEM) [38], a kinetic study and Steady-State Isotopic Transient Kinetic Analysis (SSTIKA) [39].

\* Corresponding author.

E-mail address: [K.P.deJong@uu.nl](mailto:K.P.deJong@uu.nl) (K.P. de Jong).

## 2. Materials and methods

### 2.1. Preparation

Niobium oxide hydrate (HY-340, AD/4465, 72.6 wt% Nb<sub>2</sub>O<sub>5</sub>, LOI 26.7 wt%, purity data see Supporting Information) was obtained from Companhia Brasileira de Metalurgia e Mineração – CBMM and calcined at 600 °C (5 °C min<sup>−1</sup>, 2 h) in stagnant air to obtain crystalline Nb<sub>2</sub>O<sub>5</sub> (T-phase, S<sub>BET</sub>: 16 m<sup>2</sup> g<sup>−1</sup>, PV: 0.06 mL g<sup>−1</sup>). γ-Al<sub>2</sub>O<sub>3</sub> (Sasol, Puralox SSCa-5/200, S<sub>BET</sub>: 185 m<sup>2</sup> g<sup>−1</sup>, PV: 0.5 mL g<sup>−1</sup>) and α-Al<sub>2</sub>O<sub>3</sub> (BASF, S<sub>BET</sub>: 7 m<sup>2</sup> g<sup>−1</sup>, PV: 0.015 mL g<sup>−1</sup>) were used as received. For physisorption isotherms and pore size distributions, see SI Fig. S1.

Supports were sieved to 75–150 μm and dried at ~80 °C for 1 h in dynamic vacuum. Cobalt was deposited by impregnation [40] in static vacuum (10<sup>−2</sup> bar) under mechanical mixing at room temperature with an aqueous 4.0 M Co(NO<sub>3</sub>)<sub>2</sub> solution or by co-impregnation with an aqueous 4.0 M Co(NO<sub>3</sub>)<sub>2</sub>, 0.03 M Pt(NH<sub>3</sub>)<sub>4</sub> (NO<sub>3</sub>)<sub>2</sub> (Co/Pt = 140) solution, aiming for a cobalt loading of 2–8 mg<sub>Co</sub> m<sup>−2</sup>. 2.0 g Nb<sub>2</sub>O<sub>5</sub> was impregnated with 0.54 mL, and 2.0 g α-Al<sub>2</sub>O<sub>3</sub> was impregnated with 0.55 mL of the precursor solution. 3.0 g γ-Al<sub>2</sub>O<sub>3</sub> was, in two subsequent cycles impregnated with 4.6 mL of the precursor solution, and each impregnation was followed by drying and calcination (vide infra). Impregnated volumes were up to a factor of 5 (Nb<sub>2</sub>O<sub>5</sub>) and 18 (α-Al<sub>2</sub>O<sub>3</sub>) higher than the pore volume determined using N<sub>2</sub> physisorption (SI, Fig. S1); however, all catalysts remained dry during impregnation, indicating porosity was mainly present in macropores (>50 nm). After drying overnight at 60 °C in stagnant air, the cobalt nitrate precursor was calcined at 350 °C (3 °C min<sup>−1</sup>, 2 h) in a 1 L min<sup>−1</sup> g<sub>sample</sub><sup>−1</sup> N<sub>2</sub> flow. Cobalt loading is expressed as the mass of metallic cobalt per gram of reduced catalyst. An overview of the prepared catalysts can be found in Table 1.

### 2.2. Characterization

Samples were analyzed after cobalt nitrate decomposition as described above (calcined) and after reduction at 350 °C, 3 °C min<sup>−1</sup>, 2 h in 25 vol% H<sub>2</sub>/N<sub>2</sub> (GHSV 60 × 10<sup>3</sup> h<sup>−1</sup>) and subsequent exposure to air at room temperature (passivated).

Environmental Powder X-ray diffraction (XRD) patterns were measured using a Bruker-AXS D8 Advance X-ray diffractometer using Co Kα radiation (λ = 1.789 Å). Calcined and passivated samples were analyzed in air at room temperature and heated to 350 °C (5 °C min<sup>−1</sup>, 2 h) in 25 vol% H<sub>2</sub>/He (Co/γ-Al<sub>2</sub>O<sub>3</sub>: 500 °C) in the X-ray diffractometer.

TEM samples were prepared by dry dispersion of the passivated catalyst onto a Mo grid with a holey carbon supporting film. TEM analysis was performed using an FEI Titan ETEM G2 microscope described before [38]. Samples were observed in vacuum at room temperature and in 100 Pa H<sub>2</sub> at 350 °C, microscope was operated at 300 kV, and elemental analysis was performed using Scanning

Transmission Electron Microscopy-Electron Energy Loss Spectroscopy (STEM-EELS).

Temperature programmed reduction (TPR) experiments were performed using a Micromeritics Autochem 2920 instrument. 25–100 mg calcined catalyst (6–7 mg Co) was dried at 120 °C for 1 h in an Ar flow and reduced up to 1000 °C (10 °C min<sup>−1</sup>) in a 5 vol% H<sub>2</sub>/Ar flow.

H<sub>2</sub> chemisorption measurements were performed using a Micromeritics ASAP 2020 instrument. 50–200 mg calcined catalyst was dried for 1 h in dynamic vacuum at 100 °C and reduced in an H<sub>2</sub> flow at 350 °C, 1 °C min<sup>−1</sup> for 2 h, (Co/γ-Al<sub>2</sub>O<sub>3</sub>: 500 °C). H<sub>2</sub> adsorption isotherms were measured at 150 °C, as recommended by Reuel for supported cobalt particles [41]. For all catalysts, metallic cobalt-specific surface area and average particle size were calculated assuming full reduction to Co<sup>0</sup>, a surface stoichiometry H/Co = 1 and an atomic cross-sectional area of 0.0662 nm<sup>2</sup>.

CO chemisorption measurements were performed in a setup described before [42]. 30–100 mg calcined catalyst (75–150 μm) diluted with an equal mass of SiC was reduced at 350 °C, 5 °C min<sup>−1</sup>, for 2 h (Co/γ-Al<sub>2</sub>O<sub>3</sub>: 500 °C) in 10 mL min<sup>−1</sup> H<sub>2</sub>. The amount of reversibly adsorbed CO was determined from a <sup>12</sup>CO/Ar to <sup>13</sup>CO/Kr switch (1.5/33.5 mL min<sup>−1</sup>) at 100 °C, 1.85 bar. Effluent gas was analyzed using a Balzers QMG 422 Quadrupole mass spectrometer. Surface residence time (τ<sub>CO</sub>) was determined by integration of the normalized transient curve: τ<sub>i</sub> = ∫<sub>0</sub><sup>∞</sup> F<sub>i</sub>(t) dt and was corrected for gas phase hold-up using the Ar signal. Amount of reversibly adsorbed CO (N<sub>CO,total</sub>) was calculated using the CO inlet flow (Q<sub>CO,in</sub>): N<sub>CO,total</sub> = τ<sub>CO</sub> × Q<sub>CO,in</sub>.

### 2.3. Fischer Tropsch synthesis

Catalyst testing at 1 bar was performed using a U-shaped, continuous down-flow, fixed bed reactor system. 10–50 mg calcined catalyst (75–150 μm) was diluted with 200 mg SiC (200–400 μm) and loaded in a glass reactor, ID = 3 mm, to achieve a bed height of 2 cm. 500 mg SiC was loaded on top of the catalyst bed to ensure gas preheating. A thermocouple was placed in the catalyst bed to control temperature, and deviation from target temperature was <1 °C. The catalysts were reduced at atmospheric pressure in a 33 vol% H<sub>2</sub>/Ar flow, GHSV 1.7 × 10<sup>5</sup> – 3.7 × 10<sup>5</sup> h<sup>−1</sup>, at 350 °C, 5 °C min<sup>−1</sup>, for 2 h (Co/γ-Al<sub>2</sub>O<sub>3</sub>: 500 °C). After cooling to 220 °C the gas stream was switched to synthesis gas, H<sub>2</sub>/CO = 2.0 v/v, GHSV 25 × 10<sup>3</sup> – 100 × 10<sup>3</sup> h<sup>−1</sup>, CO conversion 1–5%. Products up to C<sub>18</sub> were analyzed using an online Varian 430-GC equipped with FID. Activity and selectivity were calculated based on the hydrocarbons formed. The reported catalyst performance was determined after at least 15 h on stream. A kinetic study was performed in this setup, H<sub>2</sub> flow (4–8 mL min<sup>−1</sup>, p<sub>H2</sub> = 0.27–0.53 bar) and CO flow (2–4 mL min<sup>−1</sup>, p<sub>CO</sub> = 0.13–0.27 bar) were varied independently, and total gas flow was kept constant at 15 mL min<sup>−1</sup> by addition of Ar (4–8 mL min<sup>−1</sup>). H<sub>2</sub> and CO reaction orders (Y and Z, respectively) and pre-exponential factor k' were determined from the

**Table 1**

Cobalt loading based on intake, number of reversible CO adsorption sites determined using CO chemisorption at 100 °C (N<sub>CO,total</sub>), adsorbed amount of H<sub>2</sub> (N<sub>H2</sub>) and apparent Co particle size (d<sub>Co</sub>, H<sub>2</sub>) determined using H<sub>2</sub> chemisorption and estimated Co particle size from environmental TEM (d<sub>Co</sub>, TEM).

|                                       | Co loading |                                     | N <sub>CO,total</sub><br>(mmol <sub>CO</sub> g <sub>Co</sub> <sup>−1</sup> ) | N <sub>H2</sub><br>(mmol <sub>H2</sub> g <sub>Co</sub> <sup>−1</sup> ) | d <sub>Co</sub> , H <sub>2</sub><br>(nm) | d <sub>Co</sub> , TEM<br>(nm) |
|---------------------------------------|------------|-------------------------------------|------------------------------------------------------------------------------|------------------------------------------------------------------------|------------------------------------------|-------------------------------|
|                                       | (wt%)      | (mg <sub>Co</sub> m <sup>−2</sup> ) |                                                                              |                                                                        |                                          |                               |
| Co/Nb <sub>2</sub> O <sub>5</sub>     | 5.9        | 3.9                                 | 0.28                                                                         | 0.36                                                                   | 24                                       | 9.2                           |
| PtCo/Nb <sub>2</sub> O <sub>5</sub>   | 5.9        | 3.9                                 | 0.48                                                                         | 0.45                                                                   | 19                                       | 8.7                           |
| Co/γ-Al <sub>2</sub> O <sub>3</sub>   | 28         | 2.1                                 | 0.20                                                                         | 0.45                                                                   | 19                                       |                               |
| PtCo/γ-Al <sub>2</sub> O <sub>3</sub> | 28         | 2.1                                 | 0.43                                                                         | 0.65                                                                   | 13                                       |                               |
| Co/α-Al <sub>2</sub> O <sub>3</sub>   | 6.3        | 8.4                                 | 0.38                                                                         | 0.53                                                                   | 16                                       |                               |
| PtCo/α-Al <sub>2</sub> O <sub>3</sub> | 6.0        | 8.0                                 | 0.55                                                                         | 0.62                                                                   | 14                                       |                               |

cobalt-weight normalized activity, the latter calculated from the CO conversion level ( $X_{\text{CO}}$ ), incoming CO flow ( $F_{\text{CO,in}}$ ) and the mass of reduced catalyst ( $m_{\text{cat}}$ ) using the following:  $X_{\text{CO}} * F_{\text{CO,in}} * m_{\text{cat}}^{-1} = k' * p_{\text{H}_2}^y * p_{\text{CO}}^z$ .

Catalyst testing at 20 bar was performed using an Avantium Flowrence 16 parallel, continuous flow, fixed bed reactor system. 30–175 mg calcined catalyst (75–150  $\mu\text{m}$ ) was diluted with 100–200 mg SiC (200–400  $\mu\text{m}$ ) and loaded in a stainless steel reactor, ID = 2–2.6 mm, to achieve a bed height of 4–5 cm. Catalysts were reduced at atmospheric pressure in a 25 vol%  $\text{H}_2/\text{He}$  flow, GHSV  $1.6 * 10^3 - 10 * 10^3 \text{ h}^{-1}$ , at 350 °C,  $1^\circ\text{C min}^{-1}$ , for 8 h ( $\text{Co}/\gamma\text{-Al}_2\text{O}_3$ : 500 °C). After cooling to 180 °C the gas stream was switched to synthesis gas,  $\text{H}_2/\text{CO} = 2.0 \text{ v/v}$ , GHSV  $1.8 * 10^3 - 12 * 10^3 \text{ h}^{-1}$ , and the reactors were pressurized to 20 bar and subsequently heated to 220 °C ( $1^\circ\text{C min}^{-1}$ ) to allow for pore filling with the liquid hydrocarbon products. The GHSV was adjusted to obtain 20–30% CO conversion. Products up to  $\text{C}_9$  were analyzed using an online Agilent Technologies 7890A gas chromatograph. The reported catalyst performance was determined after at least 100 h on stream. The GHSV was defined as the total gas flow divided by the catalyst volume. Apparent turnover frequencies ( $\text{TOF}_{\text{app}}$ ) based on  $\text{H}_2$  chemisorption data (Table 1) were determined from the CO conversion level ( $X_{\text{CO}}$ ), incoming CO flow ( $F_{\text{CO,in}}$ ), the mass of reduced catalyst ( $m_{\text{cat}}$ ) and the adsorbed amount of  $\text{H}_2$  ( $N_{\text{H}_2}$ , Table 1) using the following:  $\text{TOF}_{\text{app}} = X_{\text{CO}} * F_{\text{CO,in}} * m_{\text{cat}}^{-1} * 0.5 * N_{\text{H}_2}^{-1}$ .

Steady State Isotopic Transient Kinetic Analysis (SSITKA) measurements and data treatment were performed as described before [42]. 30–100 mg calcined catalyst (75–150  $\mu\text{m}$ ) diluted with an equal mass of SiC was reduced at 350 °C,  $5^\circ\text{C min}^{-1}$ , for 2 h ( $\text{Co}/\gamma\text{-Al}_2\text{O}_3$ : 500 °C) in a  $10 \text{ mL min}^{-1} \text{ H}_2$  flow. CO and  $\text{CH}_4$  transient curves were determined from a  $^{12}\text{CO}/\text{H}_2/\text{Ar}$  to  $^{13}\text{CO}/\text{H}_2/\text{Kr}$  switch ( $1.5/15/33.5 \text{ mL min}^{-1}$ ) at 210 °C, 1.85 bar after at least 15 h at these conditions. Effluent gas was analyzed using a Balzers QMG 422 Quadrupole mass spectrometer and using a GC–MS (Agilent GC7890B – MSD5977A) equipped with TCD, FID and MSD detectors.

### 3. Results and discussion

An overview of the catalysts used in this study is shown in Table 1.

Using XRD at ambient conditions no crystalline cobalt phases were observed for calcined or passivated  $\text{Co}/\text{Nb}_2\text{O}_5$  and  $\text{PtCo}/\text{Nb}_2\text{O}_5$  catalysts. Also after reduction at 350 °C in the X-ray diffractometer no crystalline cobalt phases were observed for  $\text{Co}/\text{Nb}_2\text{O}_5$  and  $\text{PtCo}/\text{Nb}_2\text{O}_5$ , even after application of higher cobalt loadings by double impregnation ( $\sim 10 \text{ wt\%}$ , SI, Fig. S2), whereas for  $\text{Co}/\gamma\text{-Al}_2\text{O}_3$  and  $\text{PtCo}/\gamma\text{-Al}_2\text{O}_3$  the reduction of  $\text{Co}_3\text{O}_4$  to crystalline  $\text{Co}^0$  was observed at these conditions (Fig. 1). Overlap of diffraction lines with  $\text{Nb}_2\text{O}_5$  lines impedes detection of weak cobalt and cobalt oxide diffraction lines. The absence of crystalline cobalt oxide diffraction lines in  $\text{Nb}_2\text{O}_5$ -supported catalysts is in line with XRD observations by Noronha et al. [29].

TEM imaging of calcined  $\text{Co}/\text{Nb}_2\text{O}_5$  catalysts showed that cobalt was present in anisotropically shaped particles in the pores between the  $\text{Nb}_2\text{O}_5$  particles, see SI Fig. S3. After reduction and passivation restructuring of cobalt had occurred into anisotropic cobalt oxide particles on the  $\text{Nb}_2\text{O}_5$  surface (Fig. 2, left). Upon exposure to  $\text{H}_2$  at 350 °C in the electron microscope, spherical metallic cobalt particles of  $\sim 9 \text{ nm}$  were formed as shown in Fig. 2, right. Reduction was confirmed using STEM–EELS (SI, Fig. S7). For  $\text{PtCo}/\text{Nb}_2\text{O}_5$  (SI, Fig. S8), similar morphology and restructuring were observed. Based on the current study no evidence was found for a large cobalt particle size difference between  $\text{Co}/\text{Nb}_2\text{O}_5$  and

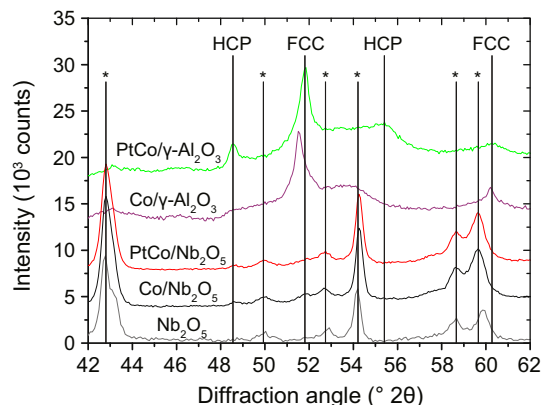


Fig. 1. Environmental X-ray diffractograms (Co  $K\alpha$  radiation) at 350 °C in 25 vol%  $\text{H}_2/\text{He}$  ( $\text{Co}/\gamma\text{-Al}_2\text{O}_3$ : 500 °C) for (Pt) 28 wt%  $\text{Co}/\gamma\text{-Al}_2\text{O}_3$  and (Pt) 6 wt%  $\text{Co}/\text{Nb}_2\text{O}_5$ .  $\text{Nb}_2\text{O}_5$  lines (\*) and hcp and fcc Co lines are indicated [43].

$\text{PtCo}/\text{Nb}_2\text{O}_5$ , for cobalt particle size distributions see SI, Fig. S9. The larger surface tension of metallic cobalt in combination with the higher mobility of metal atoms leads to these rounded off particles and can only be clearly observed using environmental TEM [44,45].

Based on the literature [6], TPR results (SI, Fig. S11) and from environmental TEM results (vide supra), full reduction was expected for all catalysts except  $\text{Co}/\gamma\text{-Al}_2\text{O}_3$  (degree of reduction  $\sim 60\%$ ). Using  $\text{H}_2$  chemisorption, an increased number of adsorption sites was observed upon Pt-promotion (Table 1) due to facilitated cobalt oxide reduction (TPR, SI Fig. S11), in line with previous reports [30–33]. Remarkably also for  $\text{PtCo}/\text{Nb}_2\text{O}_5$  a higher number of active sites was observed than for  $\text{Co}/\text{Nb}_2\text{O}_5$  although full reduction at 350 °C is expected without Pt present. For  $\text{Nb}_2\text{O}_5$ -supported catalysts a larger cobalt particle size (19–24 nm) was calculated than expected based on environmental TEM ( $\sim 9 \text{ nm}$ ) probably due to coverage of cobalt sites by  $\text{NbO}_x$  and consequent decrease in the number of metallic cobalt surface sites available for chemisorption.

To prevent underestimation of the number of active sites for  $\text{Nb}_2\text{O}_5$ -supported catalysts due to SMSI, a more accurate method to estimate the number of sites active in Fischer Tropsch catalysis might be CO chemisorption [42]. An increase in the amount of reversibly adsorbed CO per unit weight of cobalt was observed upon Pt-promotion of  $\text{Co}/\text{Nb}_2\text{O}_5$ ,  $\text{Co}/\gamma\text{-Al}_2\text{O}_3$  and  $\text{Co}/\alpha\text{-Al}_2\text{O}_3$ , respectively (Table 1). However, a wide range of surface stoichiometries has been reported between adsorbed CO and surface cobalt, as well as restructuring of cobalt during Fischer Tropsch synthesis, impeding correlation between the adsorbed amount of CO and the number of cobalt surface atoms [46–48]. For this reason, adsorbed amounts of CO and calculated TOF based on CO chemisorption data are only useful for relative comparison and should not be used for determination of absolute values of the TOF.

Catalyst selectivity (Fig. 3) and activity (Fig. 4) were evaluated in Fischer Tropsch synthesis at 1 and 20 bar (more data are available in SI, Tables S2 and S3). Furthermore, Table 2 shows results from the kinetic study investigating the influence of support and Pt-promotion on the  $\text{H}_2$  and CO reaction order and the SSITKA study performed to determine surface coverages and turnover frequencies (Full data in SI, Figs. S15–S18).

In Fischer Tropsch synthesis at 1 bar superior  $\text{C}_5+$  selectivities were observed for  $\gamma\text{-Al}_2\text{O}_3$  and  $\text{Nb}_2\text{O}_5$ -supported catalysts, compared to  $\alpha\text{-Al}_2\text{O}_3$ -supported catalysts (Fig. 3, left). For  $\text{Nb}_2\text{O}_5$ -supported catalysts, this is thought to be related to SMSI as also reported by Mendes et al. [25–29]. Upon Pt-promotion decreased  $\text{C}_5+$  selectivities were observed due to increased hydrogenation

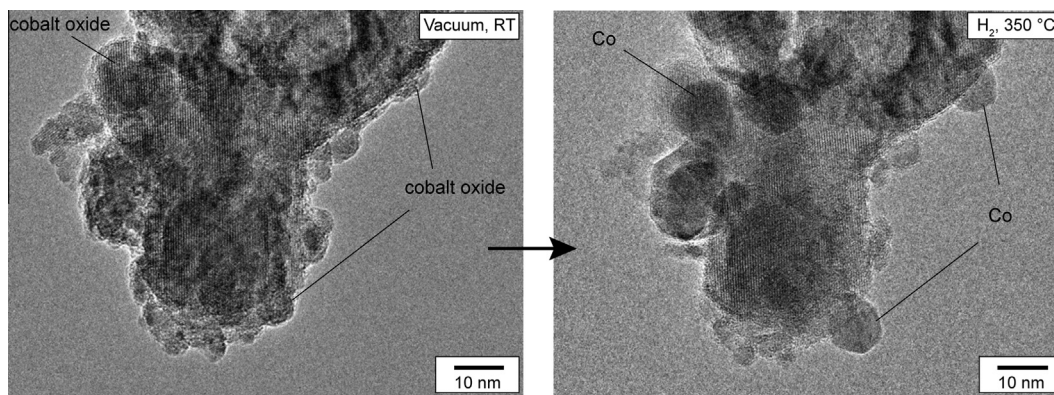


**Fig. 2.** Bright field TEM images in vacuum at room temperature (left) and in 100 Pa  $H_2$  at 350 °C (right) for  $Co/Nb_2O_5$  after ex situ reduction and passivation.

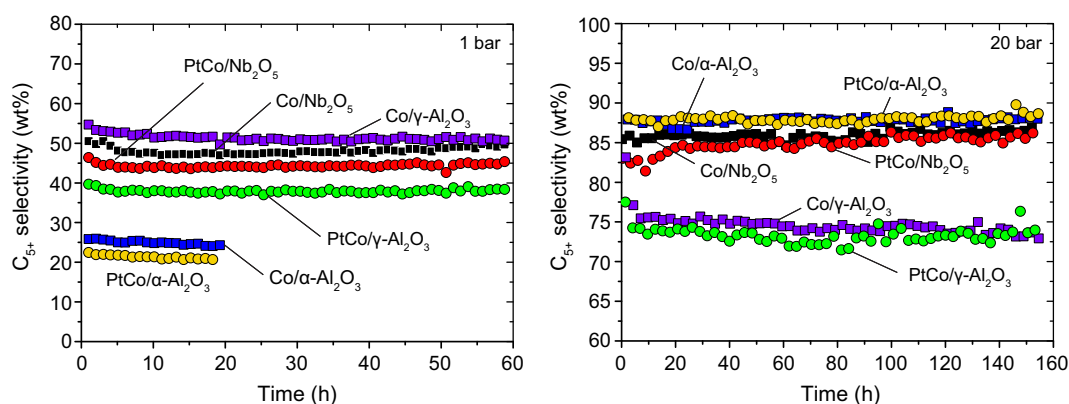


**Fig. 3.**  $C_{5+}$  selectivity in Fischer Tropsch synthesis at 1 bar, CO conversion 1–5% (left) and 20 bar, CO conversion 21–34% (right), 220 °C,  $H_2/CO = 2.0$  v/v for (Pt)Co/ $Nb_2O_5$ , (Pt)Co/ $\gamma-Al_2O_3$  and (Pt)Co/ $\alpha-Al_2O_3$  catalysts.

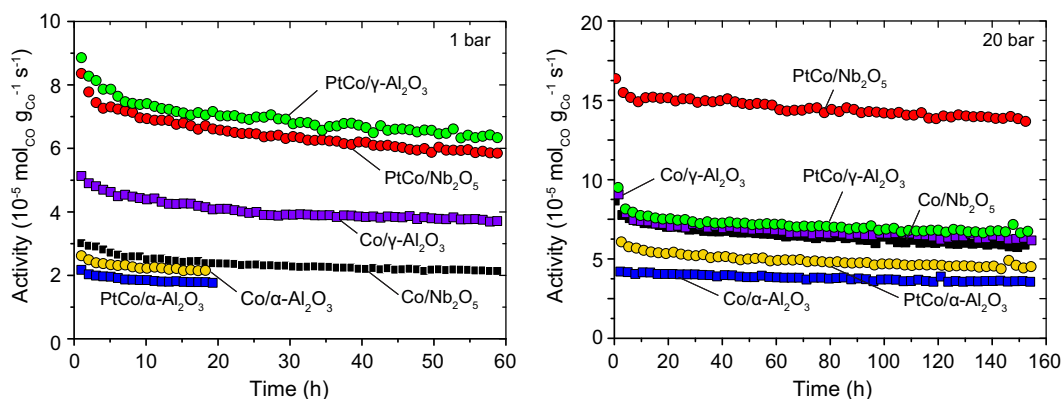


**Fig. 4.** Cobalt-weight normalized activity in Fischer Tropsch synthesis at 1 bar, CO conversion 1–5% (left) and 20 bar, CO conversion 21–34% (right), 220 °C,  $H_2/CO = 2.0$  v/v for (Pt)Co/ $Nb_2O_5$ , (Pt)Co/ $\gamma-Al_2O_3$  and (Pt)Co/ $\alpha-Al_2O_3$  catalysts.

activity, as also inferred from the increasing paraffin-to-olefin ratio (SI, Table S2). At 20 bar, superior  $C_{5+}$  selectivities were observed for catalysts supported by  $\alpha-Al_2O_3$  and  $Nb_2O_5$  compared to  $\gamma-Al_2O_3$  (Fig. 3, right). The positive relation between pore diameter and  $C_{5+}$  selectivity was previously reported by e.g. Holmen et al. and was attributed to cobalt particle size and diffusion effects [5,10,49,50]. At 20 bar, no large influence of Pt on the  $C_{5+}$  selectivity was observed (Fig. 3, right). Pressure-dependent influence of niobia on the catalyst selectivity was previously observed for niobia-promoted catalysts [8] in line with reports on MnO-promoted catalysts [13,17].

At 1 bar, the cobalt weight-normalized activity of  $Co/\gamma-Al_2O_3$  and  $Co/Nb_2O_5$  was found to increase by a factor of 1.7 and 2.8 upon Pt-promotion (Fig. 4, left). For  $Co/\alpha-Al_2O_3$ , low activity and only slight influence of Pt-promotion were observed at 1 bar. At 20 bar, no large influence of Pt-promotion on the cobalt-weight normalized activity of  $Co/\gamma-Al_2O_3$  and  $Co/\alpha-Al_2O_3$  was observed, whereas for  $Co/Nb_2O_5$ , a factor of 2.4 increase in the activity per unit weight of cobalt was observed (Fig. 4, right).

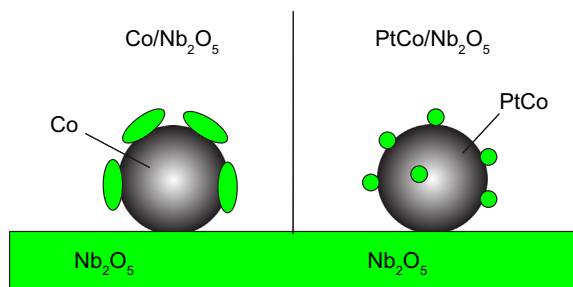
Apparent turnover frequencies were calculated based on  $H_2$  chemisorption data and are presented in Table 2. Upon Pt-promotion of  $Co/\gamma-Al_2O_3$ ,  $TOF_{app}$  at 20 bar was calculated to



**Table 2**

Apparent turnover frequency (TOF<sub>app</sub>) in Fischer Tropsch synthesis at 20 bar, 220 °C, H<sub>2</sub>/CO = 2.0 v/v, with the number of active sites based on H<sub>2</sub> chemisorption results. Reaction orders in H<sub>2</sub> and CO and pre-exponential factor (*k'*) determined in a kinetic study at 1 bar, 220 °C. Surface coverage (*θ*) and TOF determined from a <sup>12</sup>CO/H<sub>2</sub>/Ar to <sup>13</sup>CO/H<sub>2</sub>/Kr switch during SSITKA at 210 °C, 1.85 bar, H<sub>2</sub>/CO = 10 v/v, the number of active sites based on CO chemisorption results.

| Catalyst                              | FT 20 bar<br>TOF <sub>app</sub><br>(s <sup>-1</sup> ) | Kinetic study  |       |                                                                                 | SSITKA                 |                                    |                           |
|---------------------------------------|-------------------------------------------------------|----------------|-------|---------------------------------------------------------------------------------|------------------------|------------------------------------|---------------------------|
|                                       |                                                       | Reaction order |       | <i>k'</i><br>(mol <sub>CO</sub> g <sub>Co</sub> <sup>-1</sup> s <sup>-1</sup> ) | <i>θ</i> <sub>CO</sub> | <i>θ</i> <sub>CH<sub>x</sub></sub> | TOF<br>(s <sup>-1</sup> ) |
|                                       |                                                       | H <sub>2</sub> | CO    |                                                                                 |                        |                                    |                           |
| Co/Nb <sub>2</sub> O <sub>5</sub>     | 0.083                                                 | 0.73           | 0.13  | 3.5 × 10 <sup>-5</sup>                                                          | 0.67                   | 0.07                               | 0.021                     |
| PtCo/Nb <sub>2</sub> O <sub>5</sub>   | 0.15                                                  | 0.62           | 0.15  | 6.0 × 10 <sup>-5</sup>                                                          | 0.60                   | 0.07                               | 0.034                     |
| Co/γ-Al <sub>2</sub> O <sub>3</sub>   | 0.071                                                 | 0.71           | 0.05  | 2.6 × 10 <sup>-5</sup>                                                          | 0.61                   | 0.09                               | 0.024                     |
| PtCo/γ-Al <sub>2</sub> O <sub>3</sub> | 0.053                                                 | 0.81           | 0.07  | 4.4 × 10 <sup>-5</sup>                                                          | 0.53                   | 0.11                               | 0.023                     |
| Co/α-Al <sub>2</sub> O <sub>3</sub>   | 0.034                                                 | 0.91           | -0.24 | 1.5 × 10 <sup>-5</sup>                                                          | 0.66                   | 0.07                               | 0.013                     |
| PtCo/α-Al <sub>2</sub> O <sub>3</sub> | 0.037                                                 | 0.91           | -0.26 | 1.9 × 10 <sup>-5</sup>                                                          | 0.62                   | 0.06                               | 0.013                     |

**Fig. 5.** Envisaged structural model on the role of Pt in Co/Nb<sub>2</sub>O<sub>5</sub> catalysts.

decrease, whereas it remained unchanged in Fischer Tropsch synthesis at low pressure (SI, Table S2). The reason might be related to incomplete reduction of Co/γ-Al<sub>2</sub>O<sub>3</sub> during H<sub>2</sub> chemisorption experiments and consequent overestimation of TOF<sub>app</sub> after further reduction during Fischer Tropsch synthesis [51]. Upon Pt-promotion of Co/Nb<sub>2</sub>O<sub>5</sub>, TOF<sub>app</sub> was calculated to increase by a factor of 1.8 (20 bar, Table 2) to 2.2 (1 bar, SI, Table S2).

To investigate the origin of the unique activity increase upon Pt-promotion of Co/Nb<sub>2</sub>O<sub>5</sub>, a kinetic study was performed at 1 bar in which H<sub>2</sub> and CO reaction orders and the effect of Pt addition thereon were studied (Table 2). For catalysts supported by γ-Al<sub>2</sub>O<sub>3</sub> and Nb<sub>2</sub>O<sub>5</sub> higher reaction orders in CO and lower orders in H<sub>2</sub> were observed compared to α-Al<sub>2</sub>O<sub>3</sub>-supported catalysts (SI, Fig. S15) which might be related to the superior C<sub>5+</sub> selectivity for (Pt)Co/Nb<sub>2</sub>O<sub>5</sub> and (Pt)Co/γ-Al<sub>2</sub>O<sub>3</sub> compared to (Pt)Co/α-Al<sub>2</sub>O<sub>3</sub>. No large influence of Pt on the CO and H<sub>2</sub> reaction orders for the supported Co catalysts studied was observed (Table 2). The pre-exponential factor (*k'*) however was found to increase a factor of 1.7 upon Pt-promotion of γ-Al<sub>2</sub>O<sub>3</sub>- and Nb<sub>2</sub>O<sub>5</sub>-supported catalysts, indicating an increased number of active sites. Furthermore, only slight influence of H<sub>2</sub> pressure on chain growth probability (*α*) was observed, whereas *α* was found to increase with increasing CO pressure for all catalysts (SI, Fig. S16).

A Steady-State Isotopic Transient Kinetic Analysis (SSITKA) study was performed during Fischer Tropsch synthesis at 210 °C, H<sub>2</sub>/CO = 10 v/v. Activity and selectivities at these conditions are shown in the Supporting information, Table S4. <sup>12</sup>CO and <sup>12</sup>CH<sub>4</sub> transients (SI, Figs. S17–S18) were investigated from a <sup>12</sup>CO/Ar/H<sub>2</sub> to <sup>13</sup>CO/Kr/H<sub>2</sub> switch after reaching steady-state as described before [42]. CH<sub>4</sub> transient curves were fitted to a single pool and double parallel pool model [52] (SI, Fig. S19 and Table S6).

Surface residence times were determined by integration of the normalized transient curve:  $\tau_i = \int_0^\infty F_i(t)dt$  and corrected for gas phase hold-up using the Ar signal. Residence times for CH<sub>4</sub>, representing surface species which would eventually produce hydrocarbons (CH<sub>x</sub>), were corrected for the chromatographic effect of CO

[53] using the following:  $\tau_{CH_x} = \tau_{CH_x,measured} - 0.5 \cdot \tau_{CO}$ . Adsorbed amounts (*N<sub>i</sub>*) were calculated from the exit flow (*Q<sub>i,exit</sub>*):  $N_i = \tau_i \cdot Q_{i,exit}$  (SI, Table S5). Surface coverages (*θ<sub>i</sub>*) and turnover frequencies (TOF) were calculated based on the number of active sites determined from CO chemisorption (*N<sub>CO,total</sub>*, Table 1) using  $\theta_i = N_i / (2 \cdot N_{CO,total})$  and  $TOF = \tau_{CH_4}^{-1} \cdot \theta_{CH_x}$ , as proposed by Frøseth et al. [42] and are presented in Table 2.

From fitting of the CH<sub>4</sub> transient curves (SI, Fig. S19 and Table S6), single pool behavior was concluded for all catalysts. This result is in line with previous reports on cobalt Fischer Tropsch catalysts [52]. CH<sub>x</sub> residence times (SI, Table S5) were found to be shorter for Nb<sub>2</sub>O<sub>5</sub>-supported catalysts (4–5 s) than for γ-Al<sub>2</sub>O<sub>3</sub>- and α-Al<sub>2</sub>O<sub>3</sub>-supported catalysts (7–8 s), indicating faster hydrogenation and desorption of hydrocarbons. For γ-Al<sub>2</sub>O<sub>3</sub>-supported catalysts higher CH<sub>x</sub> coverage and lower CO coverage were calculated than for Nb<sub>2</sub>O<sub>5</sub>- and α-Al<sub>2</sub>O<sub>3</sub>-supported catalysts (Table 2).

Upon Pt-promotion of Co/γ-Al<sub>2</sub>O<sub>3</sub>, CH<sub>x</sub> residence times and coverages were found to increase. No large influence of Pt-promotion of Co/Nb<sub>2</sub>O<sub>5</sub> or Co/α-Al<sub>2</sub>O<sub>3</sub> on CH<sub>x</sub> coverage was observed (Table 2), whereas CO surface coverages were found to decrease. This indicates higher coverage by e.g. H or OH<sub>x</sub> and consequent higher hydrogenation probability, which is in line with the increasing paraffin-to-olefin ratio observed (SI, Table S4).

TOF were calculated assuming pseudo-first order kinetics and based on the number of active sites determined using CO chemisorption (vide supra). For Co/γ-Al<sub>2</sub>O<sub>3</sub>, PtCo/γ-Al<sub>2</sub>O<sub>3</sub> and Co/Nb<sub>2</sub>O<sub>5</sub> catalysts similar turnover frequencies were calculated (~0.02 s<sup>-1</sup>, Table 2). For Co/α-Al<sub>2</sub>O<sub>3</sub> and PtCo/α-Al<sub>2</sub>O<sub>3</sub> lower TOF were calculated (~0.01 s<sup>-1</sup>, Table 2). For PtCo/Nb<sub>2</sub>O<sub>5</sub>, the TOF based on SSITKA was found to be a factor of 1.6 higher than for Co/Nb<sub>2</sub>O<sub>5</sub>. Also based on the number of active sites determined using H<sub>2</sub> chemisorption increased TOF was calculated for PtCo/Nb<sub>2</sub>O<sub>5</sub> (SI, Table S5).

Based on the current study the origin of the factor of 2.4 increase in the cobalt-weight normalized activity upon Pt-promotion of Co/Nb<sub>2</sub>O<sub>5</sub> was concluded to be a combination of an increased number of active sites by a factor of 1.7 and an increased turnover frequency by a factor of 1.6.

The current hypothesis on the origin of the increased TOF for PtCo/Nb<sub>2</sub>O<sub>5</sub> is related to the mechanism how niobia promotes cobalt. As has been proposed before in the literature [21,54–56] for NbO<sub>x</sub> (*x* < 2.5) as well as MnO<sub>x</sub>, metal oxide species migrate onto cobalt during reduction and affect the nature of the cobalt active sites [13,17]. Assuming the impact of NbO<sub>x</sub> on cobalt is short range, the interface between Co and NbO<sub>x</sub> will be most relevant for promotion. Clearly, the extent of coverage of Co by NbO<sub>x</sub> will be important as well as the size of the clusters of NbO<sub>x</sub>. If the NbO<sub>x</sub> clusters are large then interfacial sites will be limited and blocking of cobalt metal significant. The effect of Pt is tentatively assumed to be more efficient promotion of Co by NbO<sub>x</sub> for example by

formation of smaller clusters of the oxide as schematically shown in Fig. 5. Future work will involve more detailed in situ TEM and spectroscopy investigations to prove or disprove this hypothesis.

#### 4. Conclusions

Co/Nb<sub>2</sub>O<sub>5</sub> and PtCo/Nb<sub>2</sub>O<sub>5</sub> catalysts were prepared and investigated and compared to  $\gamma$ -Al<sub>2</sub>O<sub>3</sub>- and  $\alpha$ -Al<sub>2</sub>O<sub>3</sub>-supported catalysts. Using environmental XRD poor cobalt crystallinity was observed for Co/Nb<sub>2</sub>O<sub>5</sub> and PtCo/Nb<sub>2</sub>O<sub>5</sub> after reduction. Based on environmental TEM experiments no large cobalt particle size difference was observed upon Pt-promotion of Co/Nb<sub>2</sub>O<sub>5</sub>. Using CO chemisorption the number of adsorption sites was found to be a factor of 1.7 higher for PtCo/Nb<sub>2</sub>O<sub>5</sub> than for Co/Nb<sub>2</sub>O<sub>5</sub>.

In Fischer Tropsch synthesis at 1 bar and compared to  $\alpha$ -Al<sub>2</sub>O<sub>3</sub>-supported catalysts, superior C<sub>5+</sub> selectivities were observed for  $\gamma$ -Al<sub>2</sub>O<sub>3</sub>- and Nb<sub>2</sub>O<sub>5</sub>-supported catalysts, attributed to the presence of Co<sup>2+</sup> due to incomplete cobalt oxide reduction and NbO<sub>x</sub> species at the cobalt surface, respectively. At 20 bar, Nb<sub>2</sub>O<sub>5</sub>- and  $\alpha$ -Al<sub>2</sub>O<sub>3</sub>-supported catalysts were found to exhibit superior C<sub>5+</sub> selectivities of ~85 wt%, which were attributed to the larger pore sizes compared to Co/ $\gamma$ -Al<sub>2</sub>O<sub>3</sub> and PtCo/ $\gamma$ -Al<sub>2</sub>O<sub>3</sub> catalysts.

Upon Pt-promotion of Co/Nb<sub>2</sub>O<sub>5</sub> the cobalt-weight normalized activity in Fischer Tropsch catalysis at 20 bar was found to increase by a factor of 2.4, while the high C<sub>5+</sub> selectivity was maintained. A kinetic study indicated that the number of active sites had increased by a factor of 1.7, in line with data from CO chemisorption experiments although a cobalt particle size difference was not observed using environmental TEM experiments. Steady-State Isotopic Transient Kinetic Analysis showed that a combination of an increased number of active sites and an increased turnover frequency is the origin of the activity increase in Co/Nb<sub>2</sub>O<sub>5</sub> catalysts upon Pt-promotion. Pt was tentatively proposed to bring about more efficient promotion of Co by NbO<sub>x</sub> being present as smaller clusters.

#### Acknowledgments

This research was financially supported by Companhia Brasileira de Metalurgia e Mineração – CBMM. Dr. Robson Monteiro and Mr. Rogério Ribas from CBMM are acknowledged for useful discussions and for supplying niobia samples. Ms. Yanying Qi (NTNU, Trondheim, Norway) is acknowledged for assistance during SSITKA experiments. Mr. Hans Meeldijk (ultramicrotomy, TEM), Dr. Peter Munnik (ultramicrotomy, TEM), Mrs. Marjan Versluijs-Helder (XRD), Mr. Gang Wang (TPR) and Mr. Carlos Hernández Mejía (TPR) are acknowledged for assistance and execution of indicated analyses.

#### Appendix A. Supplementary material

Supplementary data associated with this article can be found, in the online version, at <http://dx.doi.org/10.1016/j.jcat.2016.05.025>.

#### References

- [1] H.M. Torres Galvis, J.H. Bitter, C.B. Khare, M. Ruitenbeek, A.I. Dugulan, K.P. de Jong, *Science* 335 (2012) 835–838.
- [2] E. Iglesia, *Appl. Catal., A* 161 (1997) 59–78.
- [3] B.H. Davis, M.L. Occelli, *Stud. Surf. Sci. Catal.* 163 (2007) 1–420.
- [4] A.Y. Khodakov, W. Chu, P. Fongarland, *Chem. Rev.* 107 (2007) 1692–1744.
- [5] Ø. Borg, S. Eri, E.A. Blekkan, S. Storsater, H. Wigum, E. Rytter, A. Holmen, *J. Catal.* 248 (2007) 89–100.
- [6] J.H. den Otter, K.P. de Jong, *Top. Catal.* 57 (2014) 445–450.
- [7] G.P. van der Laan, A.A.C.M. Beenackers, *Catal. Rev.* 41 (1999) 255–318.
- [8] J.H. den Otter, S.R. Nijveld, K.P. de Jong, *ACS Catal.* 6 (2016) 1616–1623.
- [9] D.B. Bukur, Z. Pan, W. Ma, G. Jacobs, B.H. Davis, *Catal. Lett.* 142 (2012) 1382–1387.
- [10] S. Rane, Ø. Borg, J. Yang, E. Rytter, A. Holmen, *Appl. Catal., A* 388 (2010) 160–167.
- [11] S. Rane, Ø. Borg, E. Rytter, A. Holmen, *Appl. Catal., A* 437–438 (2012) 10–17.
- [12] S. Ali, B. Chen, J.G. Goodwin, *J. Catal.* 157 (1995) 35–41.
- [13] A. Dinse, M. Aigner, M. Ulbrich, G.R. Johnson, A.T. Bell, *J. Catal.* 288 (2012) 104–114.
- [14] J.P. den Breejen, A.M. Frey, J. Yang, A. Holmen, M.M. Schooneveld, F.M.F. Groot, O. Stephan, J.H. Bitter, K.P. de Jong, *Top. Catal.* 54 (2011) 768–777.
- [15] F. Morales, E. de Smit, F.M.F. de Groot, T. Visser, B.M. Weckhuysen, *J. Catal.* 246 (2007) 91–99.
- [16] F. Morales, F.M.F. de Groot, O. Gijzeman, A.J.M. Mens, O. Stephan, B.M. Weckhuysen, *J. Catal.* 230 (2005) 301–308.
- [17] G.R. Johnson, S. Werner, A.T. Bell, *ACS Catal.* 5 (2015) 5888–5903.
- [18] T.O. Eschemann, J.H. Bitter, K.P. de Jong, *Catal. Today* 228 (2014) 89–95.
- [19] T.O. Eschemann, K.P. de Jong, *ACS Catal.* 5 (2015) 3181–3188.
- [20] R.R. Soares, A. Frydman, M. Schmal, *Catal. Today* 16 (1993) 361–370.
- [21] R.R.C.M. Silva, M. Schmal, R. Frety, J.A.J. Dalmon, *Chem. Soc. – Faraday Trans.* 89 (1993) 3975–3980.
- [22] C.D. de Souza, D.V. Cesar, S.G. Marchetti, M. Schmal, *Stud. Surf. Sci. Catal.* 167 (2007) 147–152.
- [23] A. Frydman, R.R. Soares, M. Schmal, *Stud. Surf. Sci. Catal.* 75 (1993) 2797–2800.
- [24] A.C.B. dos Santos, A.T. Pereira, E.F. Sousa-Aguiar, J.L. Moraes, K.A. de Oliveira, M. de F. Sugaya, M. Schmal, R. de S. Monteiro, V.P. Vicentini, *World Patent WO2005085390A1*, 2005.
- [25] V.R. Ahón, P.L.C. Lage, C.D. de Souza, F.M.T. Mendes, M. Schmal, *J. Nat. Gas Chem.* 15 (2006) 307–312.
- [26] F.M.T. Mendes, C.A.C. Perez, F.B. Noronha, M. Schmal, *Catal. Today* 101 (2005) 45–50.
- [27] F.M.T. Mendes, C.A.C. Perez, F.B. Noronha, D.D. Souza, D.V. Cesar, H.-J. Freund, M. Schmal, *J. Phys. Chem. B* 110 (2006) 9155–9163.
- [28] F.M.T. Mendes, A. Uhl, D.E. Starr, S. Guimond, M. Schmal, H. Kühlenbeck, S.K. Shaikhutdinov, H.-J. Freund, *Catal. Lett.* 111 (2006) 35–41.
- [29] F.B. Noronha, C.A. Perez, R. Frety, *Phys. Chem. Chem. Phys.* 1 (1999) 2861–2867.
- [30] F. Diehl, A.Y. Khodakov, *Oil Gas Sci. Technol. – Rev. l'IFP* 64 (2009) 11–24.
- [31] W.C. Conner, J.L. Falconer, *Chem. Rev.* 95 (1995) 759–788.
- [32] G. Jacobs, T.K. Das, Y. Zhang, J. Li, G. Racoillet, B.H. Davis, *Appl. Catal., A* 233 (2002) 263–281.
- [33] T.K. Das, G. Jacobs, P.M. Patterson, W.A. Conner, J. Li, B.H. Davis, *Fuel* 82 (2003) 805–815.
- [34] D. Lorito, C. Ruocco, V. Palma, A. Giroir-Fendler, F.C. Meunier, *Appl. Catal. B Environ.* (2016), <http://dx.doi.org/10.1016/j.apcatb.2016.01.037>.
- [35] E. Iglesia, S.L. Soled, R.A. Fiato, G.H. Via, *J. Catal.* 143 (1993) 345–368.
- [36] F.B. Noronha, A. Frydman, D.A.G. Aranda, C. Perez, R.R. Soares, B. Morawek, D. Castner, C.T. Campbell, R. Frety, M. Schmal, *Catal. Today* 28 (1996) 147–157.
- [37] T.O. Eschemann, J. Oenema, K.P. de Jong, *Catal. Today* 261 (2016) 60–66.
- [38] S. Takeda, H. Yoshida, *Microscopy* 62 (2013) 193–203.
- [39] C. Ledesma, J. Yang, D. Chen, A. Holmen, *ACS Catal.* 4 (2014) 4527–4547.
- [40] P. Munnik, P.E. de Jongh, K.P. de Jong, *Chem. Rev.* 115 (2015) 6687–6718.
- [41] R.C. Reuel, *J. Catal.* 85 (1984) 63–77.
- [42] V. Frøseth, S. Storsæter, Ø. Borg, E.A. Blekkan, M. Rønning, A. Holmen, *Appl. Catal., A* 289 (2005) 10–15.
- [43] V.V. Matveev, D.A. Baranov, G.Y. Yurkov, N.G. Akatiev, I.P. Dotsenko, S.P. Gubin, *Chem. Phys. Lett.* 422 (2006) 402–405.
- [44] R. Dehghan, T.W. Hansen, J.B. Wagner, A. Holmen, E. Rytter, Ø. Borg, J.C. Walmsley, *Catal. Lett.* 141 (2011) 754–761.
- [45] S. Sadasivan, R.M. Bellabarba, R.P. Toozee, *Nanoscale* 5 (2013) 11139–11146.
- [46] R.C. Reuel, C.H. Bartholomew, *J. Catal.* 85 (1984) 78–88.
- [47] J. Yang, V. Frøseth, D. Chen, A. Holmen, *Surf. Sci.* 648 (2016) 67–73.
- [48] C.J. Weststrate, I.M. Ciobica, A.M. Saib, D.J. Moodley, J.W. Niemantsverdriet, *Catal. Today* 228 (2014) 106–112.
- [49] Ø. Borg, N. Hammer, S. Eri, O.A. Lindvåg, R. Myrstad, E.A. Blekkan, M. Rønning, E. Rytter, A. Holmen, *Catal. Today* 142 (2009) 70–77.
- [50] D. Vervloet, F. Kapteijn, J. Nijenhuis, J.R. van Ommen, *Catal. Sci. Technol.* 2 (2012) 1221–1233.
- [51] M. Claeys, M.E. Dry, E. van Steen, E. du Plessis, P.J. van Berge, A.M. Saib, D.J. Moodley, *J. Catal.* 318 (2014) 193–202.
- [52] J.P. den Breejen, P.B. Radstake, G.L. Bezemer, J.H. Bitter, V. Frøseth, A. Holmen, K.P. de Jong, *J. Am. Chem. Soc.* 131 (2009) 7197–7203.
- [53] P. Biloen, J.N. Helle, F.G.A. van den Berg, W.M.H. Sachtler, *J. Catal.* 81 (1983) 450–463.
- [54] S.J. Tauster, S.C. Fung, *J. Catal.* 55 (1978) 29–35.
- [55] S.J. Tauster, S.C. Fung, R.L. Garten, *J. Am. Chem. Soc.* 100 (1978) 170–175.
- [56] G.L. Haller, D.E. Resasco, *Adv. Catal.* 36 (1989) 173–235.